Linear and nonlinear optical spectroscopies of semiconductor and metal nanocrystals

Arao Nakamura

Center for Integrated Research in Science and Engineering, and Department of Crystalline Materials Science, Nagoya University
Chikusa ku, Nagoya 464-01 Japan
Tel: 81-52-789-4450, Fax: 81-52-789-5316
e-mail: nakamura@cirse.nagoya-u.ac.jp

(Received: Feb. 5, 1997 Accepted: Mar. 7, 1997)

Abstract

Linear and nonlinear optical properties of composite materials consisting of metal or semiconductor nanocrystals and glass are investigated by means of femtosecond laser spectroscopy. In the linear absorption spectra of CdSe and CuCl nanocrystals embedded in glasses, we observe the energy shift of optical transition between confined levels of electron-hole pairs depending on crystallite sizes. Femtosecond pump and probe spectroscopic studies demonstrate characteristic features of ultrafast relaxation dynamics of photocarriers in CdSe nanocrystals depending on the size. In Cu nanocrystal-doped glass, we find the nonlinear response time in the subpicosecond time region, which is governed by the hot electron relaxation in the metal electron system.

1. Intorduction

The recent development of laser technology has enabled us to study ultrafast pheonomena in the femtosecond time region for various material systems[1]. Nonlinear optical response and relaxation dynamics of photoexcited states in semiconductors have been extensively investigated by means of various spectroscopic techniques using femtosecond pulse lasers. There is also increasing interest in the study of nano-structured semiconductors in which carriers are confined by the potential wall. In particular, the quantum well and superlattice structures of GaAs/AlGaAs have been intensively studied not only for physics in low dimensional systems but also for device applications such as optoelectronic and photonics devices.

In nanocrystals with radii of less than several tens nanometers, electrons, holes and excitons are confined three-dimensionally by the matrix potential. Theoretical studies have shown that the quantum confinement of excitons in the restricted geometry gives rise to large enhancement of the third-order optical nonlinearity[2,3]. Third-order susceptibilities $\chi^{(3)}$ ranging from 10^{-10} to $\sim 3\times10^{-8}$ esu were reported for CdSSe-doped glasses[4-8]. Nonlinear absorption measurements and degenerate four-wave mixing measurements for CuCl nanocrystals have shown that the $\chi^{(3)}$ is enhanced to 10^{-6} esu depending on the crystallite size[9-14].

The optical nonlinearity of small metal particles embedded in glass is also attractive for potential applications in nonlinear optical signal processing and optical devices because of their ultrafast response. Large picosecond optical nonlinearities have been shown for Au, Ag and Cu nanocrystals and the nonlinearity is attributed to the enhancement of the local field inside the metal nanocrystal at the surface plasmon resonance[15-18].

In this paper, we report on linear and nonlinear spectroscopic studies of composite materials consisting of metal or semiconductor nanocrystals and glass. We review quantum size effects on photoexcited electron-hole pairs and ultrafast nonlinear optical response of CdSe, CuCl and Cu nanocrystals. In linear absorption spectra, we can observe the energy shift of optical transition between confined levels depending on crystallite sizes. Furthermore, we represent ultrafast relaxation dynamics of photocarriers in CdSe nanocrystal by means of femtosecond pump and probe spectroscopy, which demonstrates size-dependent behaviors of ultrafast nonlinear absorption. In Cu nanocrystal-doped glass, we demonstrate subpicosecond time response in the optical nonlinearity, which originates from hot electron relaxation in the free electron system.

2. Experimental

We used a femtosecond pump-probe method to

investigate ultrafast relaxation dynamics of photocarriers and nonlinear response. The femtosecond pump-probe system consists of a femtosecond pulse generator, dye amplifier, a white continium generator, an optical delay and spectrometers. The picosecond pulses at the wavelength of 603 nm generated by a hybridly modelocked dye laser were compressed to 100 fs and the pulse energy was 100 μJ. The amplified pulses are divided into two beams and one was used to pump the sample. The other was focused on a D_2O cell to generate a white continium pulse, which was used to measure absorption spectrum ranging from 400 to 900 nm under the excitation by the strong pumping pulse. Changing the delay distance between the two beams, we can measure absorption spectra as a function of the time delay between the pump and probe pulses. The peak power densities of pump pulses used here were 0.3-40 GW/cm^2.

3. Quantum Size Effects in Semiconductor Nanocrystals

In nanocrystals photoexcited electrons and holes are three-dimensionally confined by the potential due to the matrix material. There are two limiting cases in the confinement effects according to the ratio of the crystallite radius R to the Bohr radius a_B of exciton[19]. For $R/a_B < 2$, an electron and a hole are individually confined, because the Coulomb energy can be neglected compared to the confinement energy. If the confinement potential is spherical and infinite, the lowest energy of an electron-hole pair is written by the following equation,

$$E = E_g + \hbar^2\pi^2/2\mu R^2 \qquad (1)$$

where E_g and μ are the band gap and the reduced mass, respectively. For $R/a_B > 4$, the exciton is weakly confined. Since the confinement energy is less than the Coulomb energy, the character of the exciton as a quasiparticle is well conserved and the translational motion is confined. In this case, the lowest energy of exciton is given by the following equation,

$$E = E_g - E_{ex} + \hbar^2\pi^2/2MR^2 \qquad (2)$$

where E_{ex} and M are the exciton binding energy and the translational mass, respectively.
The quantum size effects have been observed in various semiconductor nanocrystals. Figure 1 shows absorption spectra of CdSe nanocrystals (a_B = 45 A) measured at 2 K[21]. In CdSe nanocrystals for R < 31 A, absorption edge is shifted to the shorter wavelength side, and for radii of 21 and 18 A we observe distinct absorption peaks. These peaks are due to the optical transition of the lowest quantized level of the A (or B) valence band to the lowest level of the conduction band. The valence band of CdSe consists of A, B and C bands. This behavior indicates the individual confinement of an electron and a hole. If the crystallite radius is increased to more than 100 A, we can see the exciton peak due to the A exciton and B exciton, and the blue shift of these peaks indicates the exciton confinement.

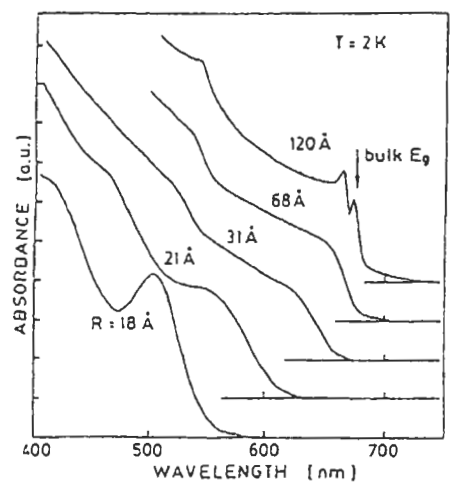

Fig. 1 Absorption spectra of CdSe nanocrystals with various radii at 2 K. The arrow indicates the band gap of the bulk crystal.

The confinement effect on the translational motion of excitons was more clearly demonstrated for CuCl nanocrystals with the Bohr radius of 6.8 A [12,20]. Figure 2 represents the absorption spectra measured for CuCl nanocrystals at 80 K[12]. The sharp and broad absorption bands are assigned to Z_3 and Z_{12} excitons coming from Γ_7 and Γ_8 valence bands and they are shifted to the higher energy sides for smaller sizes compared to the bulk energy of Z_3 exciton which is illustrated by the arrow. This behavior indicates the confinement of translational motion of excitons. Recently, however, the detailed study of confinement effects in CuCl, CuBr and their alloy nanocrystals showed that the size dependence of the exciton energies cannot be explained by

Eq.(2) but is fitted to the equation which takes into account the 1/R term in Eq.(2) [22]. The origin of the 1/R term is thought to be the Coulomb repulsive interaction which is due to the negative charge localized at the interface.

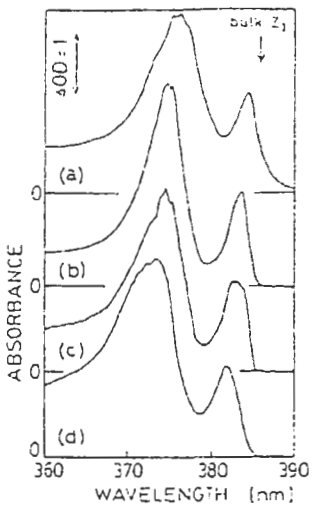

Fig. 2 Absorption spectra of CuCl nanocrystals with various radii at 77 K. The arrow indicates theZ3 exciton energy of the bulk crystal. (a) R=33 A, (b) R=28 A, (c) R=24 A, (d) R=21 A.

4. Ultrafast Carrier Relaxation in CdSe Nanocrystals

4.1 Strong Confinement Regime

We measured transient absorption spectra of CdSe nanocrystals with R=23 A, in which the individual confinement of electrons and holes takes place [21]. Figure 3(a) shows the absorption spectrum at 77 K. The weak absorption shoulder comes from the transition between the quantized states of the valence and conduction bands. Shown in Fig.3(b) are differential absorption spectra for various delay times. The differential spectrum was taken the substraction of the spectrum without pumping from that with pumping. The decrease in the absorption (bleaching) is clearly observed around 625 and 510 nm for the delay times of > 1.9 ps. The large bleaching at 625 nm corresponds to the transition from the quantized state of A(B) valence band to that of the conduction band. The weak bleaching at 510 nm is ascribed to the transition between the quantized levels of the C valence band and the conduction band.

In general, the absorption saturation is governed by the exchange interaction, state

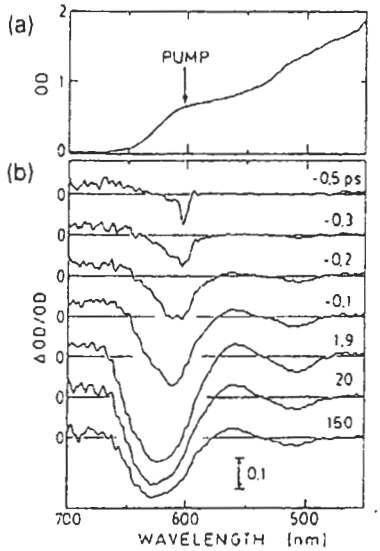

Fig. 3 (a) The absorption spectrum of CdSe nanocrystals (R=23 A) at 77 K without pumping pulses and (b) the differential absorption spectra for various delay times. DOD/OD means the absorption change divided by the optical density.

filling that is the blocking of the transition and the screening of Coulomb interaction. The exchange interaction and the state filling are due to the Pauli's exclusion principle. Since the band state is quantized to form discrete levels in nanocrystals, the exclusion principle is dominant mechanism for the absorption saturation. The large bleaching around the pumping wavelength demonstrates the zero-dimensional feature of the nonlinear absorption coming from the state filling.

Although the bleaching band around 625 nm is broad when the delay time exceeds 1.9 ps, that for the negative delay is as sharp as the spectral width of the pumping pulses, and the bleaching peak wavelength being at 603 nm corresponds to the pumping wavelength. The sharp bleaching structure observed for the negative delay is therefore thought to be a coherent spike, which is generated by the coherent effect between the pump and probe pulses.

Figure 4 shows the time evolution of the absorption changes measured at the different wavelengths. The beaching signals measured at 510 and 625 nm exhibit two-component decay behaviors with the decay times of about 40 and 400 ps. The absorption increase seen at 560 nm rises more slowly than the bleaching, and its decay time is 580 ps which is longer than that of the bleaching.

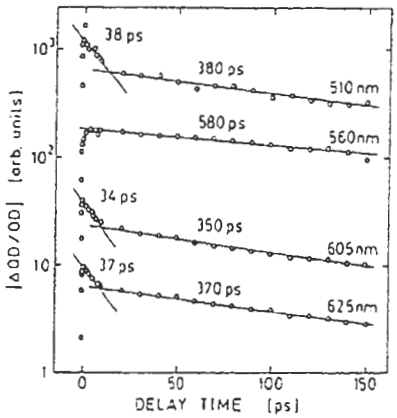

Fig. 4 Time evolution of DOD/OD at different wavelengths.

In CdSe nanocrystals embedded in glass, there exist several trapping centers which were observed by the luminescence measurements [23,24]. The shallow centers yield the emission band just below the absorption edge and the decay behavior exhibits non-exponential decay. The decay times of fast and slow components are about 200 ps and several tens nanoseconds, respectively. The emission band due to the deep centers are observed at 850 nm and its decay time is several hundreds microseconds.

Taking into account a model of the multilevel system which consists of the shallow and deep traps and the lowest quantized levels of the bands, we can explain the two-component decay behaviors. We assume that the shallow traps for electrons and holes contribute to the bleaching of the transition between the confined levels, whereas the electron and holes trapped at the deep centers do not contribute to the bleaching. The detailed analysis of the rate equations for the electrons and holes suggests that the fast recovery component is mainly governed by the trapping time of electrons and holes into the deep centers and the slow component corresponds to the electron-hole recombination time on the shallow centers.

4.2 Weak Confinement Regime

When the crystallite radius is larger than the exciton Bohr radius (45 A) of CdSe, the confinement energy becomes of the order of the binding energy of exciton. In this case we can expect the transient behavior different from that observed in the strongly confined system. To investigate relaxation dynamics of photocarriers without the exciton effect, the sample was kept at room temperature. Figure 5(a) shows the absorption spectrum of CdSe nanocrystals with R > 120 A, which exhibits the features of the band to band absorption [21]. The absorption edge is very close to the band gap for bulk crystals.

Figure 5(b) depicts the temporal change of the differential absorption spectra. The bleaching peaks around 700 and 560 nm correspond to the transitions from the A(B) valence band and the C valence band to the conduction band, respectively. Induced absorption was also observed around 620 nm between the two bleaching bands. There are two characteristic features to be noticed: First, no bleaching is observed at the pumping wavelength ,and second, the bleaching spectrum is asymmetric exhibiting the tail towards the shorter wavelength sides. These results are similar to those seen in the bulk crystals. Since the confinement energy for this sample is comparable to the thermal energy corresponding to room temperature, the discrete energy structure would be smeared out.

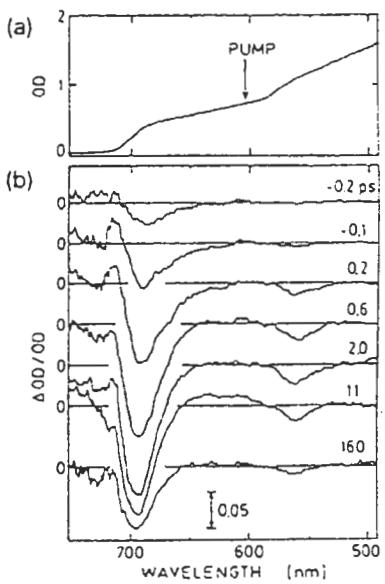

Fig. 5 (a) the absortion spectrum of CdSe nanocrystals (R>120 A) at room temperature without pumping pulses and (b) the differential absorption spectra (DOD/OD) for various delay times.

The temporal behavior of the bleaching spectrum is interpreted in terms of the energy loss and thermalization processes of photoexcited carriers. The mutual collision of carriers and the collision with the crystallite surface lead to the quasi-thermal equilibrium of carriers within the duration of the pumping pulse. If the bleaching originates from the

phase-space filling effect and the three dimensional density of state is assumed, the bleaching spectrum shape can be fitted to the Maxwell-Boltzmann distribution function. From this analysis, we can derive carrier temperatures as a function of the delay times. The obtained values of the temperatures are summarized in Fig. 6. The carrier temperature falls rapidly from 800 K to 400 K within 1 ps, and it continues to down to 350 K at 150 ps. If we consider the LO and LA phonon interactions as the cooling mechanism, the fast cooling is due to the emission of LO phonons and that of the slow component is due to that of LA phonons. The thermalization of hot carriers in the bands is nothing but the charateristic feature of the three dimensional system. Figures 3 and 5 demonstrate the clear differences between the zero-dimensional and three-dimensional behaviors of nonlinear optical response.

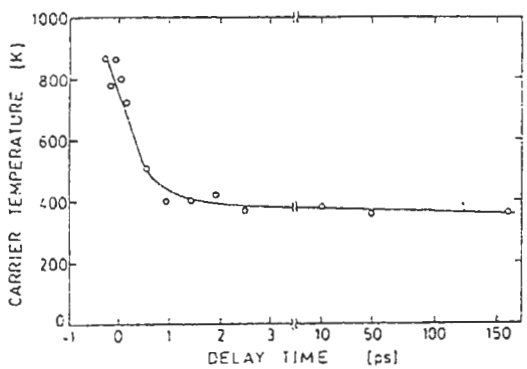

Fig. 6 The carrier temperature as a function of the delay times.

5. Ultrafast optical nonlinearity of Cu nanocrystals in glass

In metal nanocrystal-doped glasses, the nonlinear optical response is governed by the resonant behavior of the surface plasmon of free electrons. The optical excitation generates nonequilibrium electrons in the free electron system and these electrons are relaxed to the equilibrium state via the electron-phonon interaction. The thermalization process of nonequilibrium electrons would determine the response time of the nonlinearity.

Figure 7(a) shows the linear absorption spectrum of copper particles with a radius of 40 A at 300 K. A surface plasmon peak is observed at 2.2 eV and a large shoulder is due to the transition from the d band[18]. Shown in Fig.7(b) are differential absorption spectra for various delay times. The spectra exhibit a bleaching at the plasmon peak and the absorption increase emerges on the both sides of the peak, which suggests the broadening of the plasmon absorption band.

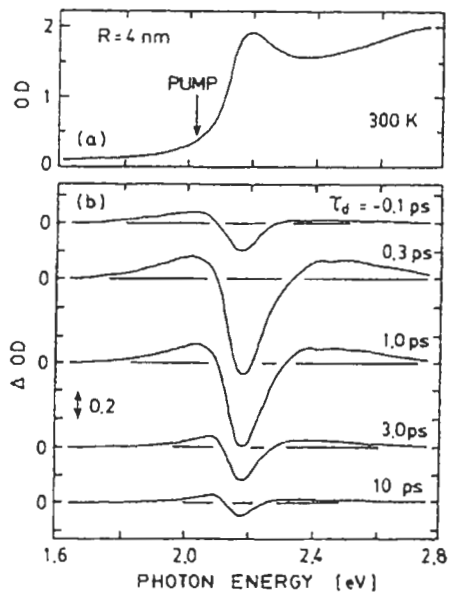

Fig. 7 (a)The linear absorption spectrum of copper nanocrystals with a radius of 40 A at room temperature, (b)the differential absorption spectra for various delay times.

Figure 8 shows the time response measured at the early stage of the time delay for different laser fluences[18]. The bleaching signal decreases within ~4 ps and the decay behavior is non-exponential depending on the pumping laser fluence. The bleaching for 4.0 mJ/cm^2 recovers in 4 ps, while the recovery time for 0.2 mJ/cm^2 is shortened to be ~1 ps. This behavior for the small particles is quite similar to the results of the thermomodulation observed for thin copper films by Elsayed-Ali et al.[25]. As the laser fluence was changed from 11.4 mJ/cm^2 to 1.4 mJ/cm^2, the decay time decreased from 4 ps to 1 ps. If we define the response time by the time at which the signal decays to 1/e, we obtain $\tau_{1/e}$ ~0.7 ps for 0.2 mJ/cm^2 . This demonstrates that we can achieve a subpicosecond time response for the copper particles at the lower laser level.

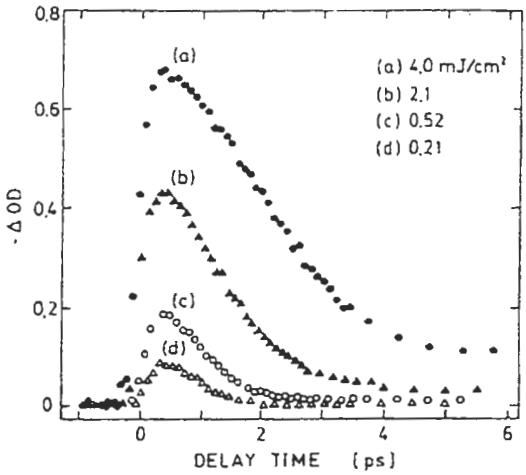

Fig. 8 The time evolution of the bleaching signal measured at 2.2 eV for various laser fluences.

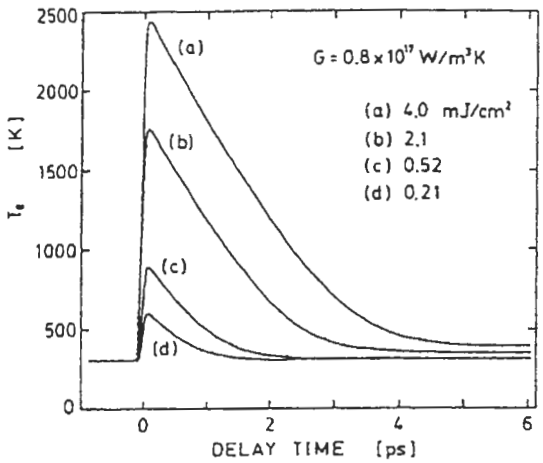

Fig. 9 The calculated electron temperatures as a function of the delay times for measured laser fluences.

We now examine the relaxation dynamics of the electron temperature by the usual electron-phonon coupling model[26]. The time evolution of the electron and the lattice temperatures, T_e and T_l, respectively, is described by the coupled differential equations:

$$C_e(T_e)\frac{\partial T_e}{\partial t} = k\Delta^2 T_e - G(T_e - T_l) + P(t) \quad (3)$$

$$C_l\frac{\partial T_l}{\partial t} = G(T_e - T_l) \quad (4)$$

where C_e (T_e) is the temperature-dependent electronic heat capacity, C_l is the lattice heat capacity, k is the thermal conductivity, G is the electron-phonon coupling constant, P(t) is the excitation energy density per unit time and unit volume in a particle.

In Fig. 9 we show the calculated results of the electron temperature as a function of the delay time for the pumping fluences of 0.21, 0.52, 2.1, 4.0 and 10 mJ/cm^2 used in the experiments. We used the values of C_e and C_l for the bulk Cu crystal and the value of G = 0.8×10^{17} W/m^{3}K, which is slightly smaller than that for the thin film(~1×10^{17} W/m^{3}K)[25]. The observed decay behavior depending on the pumping fluence can be well reproduced by this model. The response times are 2.7, 1.4, 1.0, 0.7 ps for the fluences of 4.0, 2.1, 0.52 and 0.21 mJ/cm^2, and we can obtain the subpicosecond time response for the lower pumping fluences.

It is worthy to note that the shorter response time is achieved when the pumping fluence is decreased. This is the characteristic feature of metal nanocrystal-doped glasses. In semiconductor-doped glasses, the response time is either independent of the pumping intensity or lengthened for the lower intensities, because the response time is determined by the trapping time of carriers.

6. Summary

We have investigated the quantum size effects and the ultrafast nonlinear optical response of semiconductor and metal nanocrystals embedded in glasses. Quantum size effects on photoexcited electrons and holes were demonstrated for CdSe and CuCl nanocrystals. In nanocrystals for $R < a_B$, electrons and holes are individually confined, while the translational motion of excitons is confined for $R > a_B$. We have found clear differences between the carrier relaxation processes in these confinement regimes. In the small nanocrystals, the bleaching is ascribed to the state-filling effect of the quantized states and to the exchange effect due to the trapping states. In the large nanocrystals, the cooling dynamics of photocarriers are observed exhibiting three-dimensional features. The ultrafast nonlinear response of Cu nanocrystals has been also investigated. The response time is as short as 0.7 ps, which is governed by the cooling dynamics of hot electrons in the metal electron system.

Acknoledgements

This work was supported by the Grant-in-Aid for Scientific Research from the Japanese Ministry of Education, Science, Sports and Culture and the New Energy and Industrial Technology Development Organization

(NEDO).

References

1. Ultrafast Laser Pulses and Applications, ed. W. Kaiser, Springer-Verlag Berlin, 1988.
2. E. Hanamura, Phys. Rev. B37, 1273, (1988).
3. T. Takagahara: Phys. Rev. B39, 10206 (1989).
4. R. K. Jain and R. C. lind: J. Opt. Soc. Am. 73, 647, (1983).
5. P. Roussignol, D. Ricard, J. Lukasik and C. Flytzanis: J. Opt. soc. Am. B4, 5 (1987).
6. L. H. Acioli, A. S. L. Gomes and J. R. Rios Leite: Appl. Phys. Lett. 53, 1788, (1988).
7. J. Yumoto, H. Shinojima, N. UesugiK. Tsunetomo, H. Nasu and Y. Osaka, Appl. Phys. Lett. 57, 2393, (1990).
8. N. Finlayson, W. C. Banyai, C. T. Seaton, G. I. Stegeman, M. O'Neil, T. J. Cullen and C. Ironside, J. Opt. Soc. Am. B6, 675, (1989).
9. Y. Masumoto, M. Yamazaki and H. Sugawara, Appl. Phys. Lett. 53, 1527, (1988).
10. B. L. Justus, M. E. Seaver, J. A. Ruller and A. J. Campillo, Appl. Phys. Lett. 57, 1381, (1990).
11. A. Nakamura, T. Tokizaki, T. Kataoka, N. Sugimoto and T. Manabe, Tech. Digest Int. Quantum Electronics Conf. Anaheim, p178, (1990).
12. A. Nakamura, T. Tokizaki, H. Akiyama and T. Kataoka, J. Lum. 53, 105, (1992).
13. T. Tokizaki, T. Kataoka, A. Nakamura, N. Sugimoto and T. Manabe, Jpn. J. Appl. Phys. 32, L782, (1993).
14. T. Kataoka, T. Tokizaki and A. Nakamura, Phys. Rev. B48, 2815, (1993).
15. D. Ricard, P. Roussignol and C. Flytzanis, Opt. Lett. 10, 511, (1985).
16. M. J. Bloemer, J. W. Haus and P. R. Ashley, J. Opt. Soc. Am. B7, 790, (1990).
17. K. Uchida, S. Kaneko, S. Omi, C. Hata, H. Tanji, Y. Asahara, A. J. Ikushima, T. Tokizaki and A. Nakamura, J. Opt. Soc. Am. B11, 1236, (1994).
18. T. Tokizaki, A. Nakamura, S. Kaneko, K. Uchida, S. Omi, H. Tanji, Y. Asahara, Appl. Phys. Lett. 65, 941, (1994).
19. Al. Efros and A. L. Efros, Soviet Phys. JETP 8, 772, (1982).
20. A. I. Ekimov, Al. L. Efros, M. G. Ivanov, A. A. Onushchenko and S. K. Shumilov: Solid State Commun. 69, 565, (1989).
21. T. Tokizaki, H. Akiyama, M. Takaya and A. Nakamura, J. Crys. Growth. 117A, 603, (1992).
22. A. Nakamura, M. Ohta, S. Sasaki and M. Takata, J. Lum.
23. P. Rossignol, D. Ricard, J. Lukasik and C. Flytzanis, J., Opt. Soc. Am. B4, 5, (1987).
24. A. I. Ekimov, I. A. Kudryavtsev, M. G. Ivanov and Al. L. Efros, J. Lum. 46, 83 (1993).
25. H. E. Elsayed-Ali, T. B. Norris, M. A. Pessot and G. L. Eesley, Phys. Rev. Lett. 58, 1212, (1987).
26. S. I. Anisimov, B. L. Kapeliovich and T. L. Pere'man, Sov. Phys. JETP 39, 375, (1975).